ASTRONOMY & ASTROPHYSICS SUPPLEMENT SERIES

Astron. Astrophys. Suppl. Ser. **118,** 311-321 (1996)

Kinematics of the local universe. III. Neutral hydrogen observations of southern galaxies

H. Di Nella[1,2], G. Paturel[1], A.J. Walsh[2], L. Bottinelli[3,4], L. Gouguenheim[3,4] and G. Theureau[3]

[1] CRAL-Observatoire de Lyon, F-69561 Saint-Genis Laval Cedex, France
[2] Depart. astrophysics, Uni. New South Wales, 2052 Sydney, NSW, Australia
[3] Observatoire de Paris-Meudon, ARPEGES, URA CNRS 1757, F-92195 Meudon Principal Cedex, France
[4] Université Paris-Sud, F-91405 Orsay, France

Received January 11; accepted January 15, 1996

Abstract. — This paper is the third one in a series dedicated to the study of the kinematics of the local universe. It gives 52 new 21-cm neutral hydrogen measurements, made with the 64-m Parkes radio telescope. These new measurements are used to built a complete sample of 5,219 galaxies with 21-cm line widths, radial velocity and apparent diameter. This sample is complete down to a diameter limit of 1.6 arcmin.

Key words: galaxies: redshifts; ISM — radio lines: galaxies — catalogue

1. Introduction

The main purpose of this series of papers is the study of the velocity field from unbiased distances for a galaxy sample complete down to a given apparent diameter limit of 1.6 arcmin (i.e. $\log D_{25} = 1.20$, where D_{25} is the apparent diameter at the brightness level of 25 Bmag.arcsec^{-2}. This diameter is expressed in $0.1'$ following the convention adopted by de Vaucouleurs et al. 1976). This program has been presented previously (Paturel et al. 1990). First, it requires radial velocity measurements and then, 21-cm line width measurements, the later ones being used for distance determination through the Tully-Fisher relation (Tully & Fisher 1977). Radial velocity measurements were thus undertaken at ESO, OHP and Nançay and 21-cm line width measurements at Nançay. Because of the pointing limitation of the Nançay radio telescope[1], all galaxies in the extreme south (i.e. below -38 deg) have to be observed at Parkes. In two previous papers (Bottinelli et al. 1992; Bottinelli et al. 1993), 664 radial velocity measurements were published. In the present paper 52 new HI measurements obtained with the Parkes radio-telescope are given.

2. Observations

The observations were conducted in 1994, from August 16 to 20 with the Parkes 64-m radio telescope at Parkes Observatory, ATNF. The sensitivity is 0.63 KJy^{-1} and the receiver system temperature is 50 K. The HPBW of the telescope is $15'$. The 1024-channel autocorrelation spectrometer (Ables et al. 1975) was normally used in the $2-$*channel* mode, with each receiver sampled in 512 delay channels. Galaxies were observed with 32 MHz bandwith, which gives an effective velocity resolution of 7 km/s. Integrations of 5 minutes were made on source, followed by similar reference observation made with a declination offset of +0.5 deg. Flux scales for the HI spectra were determined in each polarization channel from observations of the continuum-radio source Hydra A (Davies et al. 1989). The flux density and spectral index ($S_\nu \sim \nu^{-\alpha}$) of this source were taken to be S_ν=43.5 Jy and α=0.90 at 1410 MHz. The linear polarization of Hydra A is negligibly small ($<$ 0.3 per cent).

3. Results

Spectra were processed with the *Spectral Line Analysis Package* (SLAP) given by Staveley-Smith (1985). Some individual bad scans were rejected after examination by eye. Then, the remaining scans were added while spectra of both polarizations are averaged. A baseline is fitted with a polynomial for reconstructing the corrected 21-cm line profile. The adopted order is decided interactively but it is generally about 3. The 21-cm line profiles are given in the last pages. Each frame is identified with the PGC name according to Table 1.

Send offprint requests to: H. Di Nella

[1]The transit meridian Nançay radiotelescope can observe for declinations in the range ≈ 90 deg to -38 deg.

The width is measured at two levels, 50% and 20% of the peak, leading to uncorrected values W_{50} and W_{20}. The systemic velocity is measured as the middle of the 20% level. It is expressed with the optical convention $c.\Delta\lambda/\lambda$. The integral flux of the calibrated profile gives the observed HI flux, $F_{\rm HI}$. The signal-to-noise ratio (S/N) is defined as: $F_{\rm HI}/(W_{20}\sigma_{\rm f})$ (Roth et al. 1994), where $\sigma_{\rm f}$ is the rms noise in Jy.

We calculated the actual internal errors on the measured heliocentric velocity (V), width at 20% ($W20$) and at 50% ($W50$), according to Fouqué et al. (1990):

$\sigma(V) = 3.3 \times 1.11 R^{0.5} P^{0.5} S^{-1}$

$\sigma(W50) = 2\sigma(V)$

$\sigma(W20) = 3\sigma(V)$

Where S is the signal to noise ratio, R the spectral resolution and $P = (W20 - W50)/2$.

From the equation:

$$\sigma^2 = \sigma(V\mathrm{literature})^2 + \sigma(V\mathrm{radio})^2$$

A comparison between literature and radio velocities shows that the slope doesn't differ significantly from one and the zero point doesn't differ significantly from zero. We obtain :

$\sigma^2 = 87$ km s^{-1}

and:

$\sigma(V\mathrm{radio}) = 7\mathrm{kms}^{-1}$

thus:

$\sigma(V\mathrm{literature}) = 87\mathrm{kms}^{-1}$

This shows that all the error in the comparison comes from the measurements of the literature. This is coherent with the fact that measurements from the literature are essentially optical measurements. This error is also in agreement with the mean error (90 km s^{-1}) on optical velocity measurements conducted for the present study (Bottinelli et al. 1992).

The detailed list of observed objects is given in Table 1. The columns are arranged as follows:

- *Column 1*: PGC Number according to Paturel et al. (1989)
- *Column 2*: Name according to a hierarchy (NGC, IC, ESO...)
- *Column 3*: 1950-RA and DEC. in hr, mn, s and deg.′,″
- *Column 4*: Heliocentric radial velocity (in km/s) from the literature
- *Column 5*: Heliocentric velocity with its error (optical convention in km/s)
- *Column 6*: Width at 20% of the peak with its error (optical convention in km/s)
- *Column 7*: Width at 50% of the peak with its error (optical convention in km/s)
- *Column 8*: HI flux integral (in Jy km s^{-1})
- *Column 9*: S/N ratio $F_{\rm HI}/(W_{20}\sigma_{\rm f})$

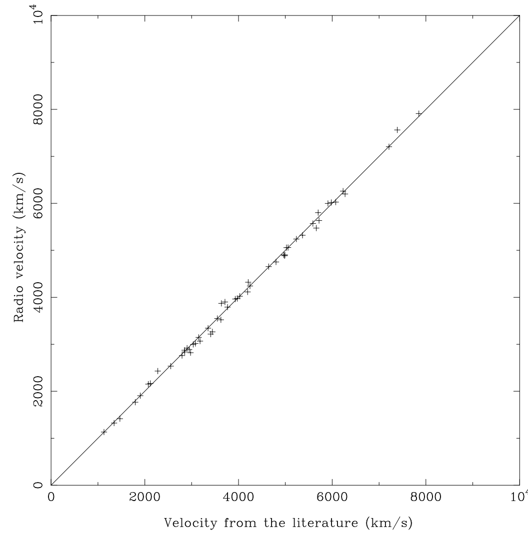

Fig. 1. Comparison between optical and radio velocities. The continuous line is the first bissect. The mean dispersion is: 87 km s^{-1}

- Column 10. Note

4. Completeness in different regions

The global completeness of the total sample of 5.219 galaxies was studied in a previous paper (Paturel et al. 1994), but we have not yet tested the completeness in different regions of the sky.

A study is conducted in the hypergalactic plane coordinates[2] *hgl*, *hgb* as defined by Di Nella & Paturel (1994). This plane contains superclusters of Perseus-Pisces, Pavo-Indus, Centaurus, Coma (and a part of the Great-Wall) and the Local Super Cluster. Two regions are studied (Fig. 2):

- On the side of Centaurus (Great Attractor, see Burstein et al. 1987), i.e. $0 \leq hgl < 180$ deg. The corresponding completeness curve is drawn with a dashed line.
- On the opposite side, i.e. $180 \leq hgl < 360$ deg. The corresponding completeness curve is drawn with a dotted line.

The completeness is well fulfilled up to the limit $\log D_{25} = 1.2$. This shows that the small deficiency in the total sample, towards the Northern and Southern poles should not affect a study of the kinematics in the so-called hypergalactic plane. However, more HI observations are still needed in the southern hemisphere.

Acknowledgements. We acknowledge L. Staveley-Smith for his support and the staff members at Parkes observatory. We received financial support for this project from the INSU (Institut National des Sciences de l'Univers) under the

[2] *hypergalactic plane* according to Paturel et al. (1988).

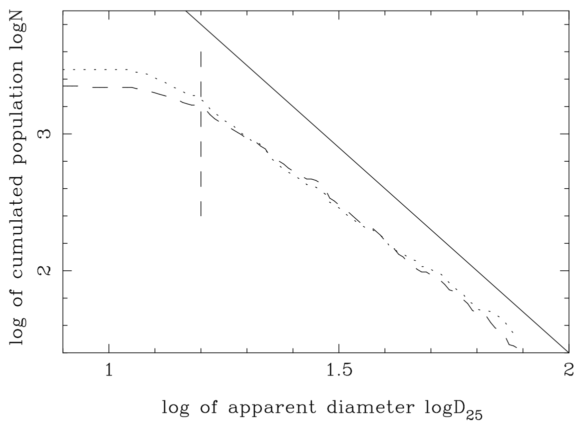

Fig. 2. Completeness curve on the side of the presumed Great-Attractor (dashed line) and on the opposite side (dotted line)

French-Australian Cooperation Scheme and from the 'Conseil Régional Rhone-Alpes' under the program: 'EURODOC'.

References

Ables J.G., Brooks J.W., Cooper B.F.C., et al., 1975, Rev. Sc. Instr. 46, 284

Bottinelli L., Durand N., Fouqué P., et al., 1992, A&AS 93, 173

Bottinelli L., Durand N., Fouqué P., et al., 1993, A&AS 102, 57

Burstein D., Davies R., Dressler A., et al., 1987 in Galaxy Distances and Deviation from the Universal Expansion. In: Madore and Tully (Reidel), p. 123

Davies R.D., Staveley-Smith L., Murray J.D., 1989, MNRAS 236, 171

Di Nella H., Paturel G., 1994, C.R.Acad.Sc. Paris, t.319, p. 57

Fouqué P., Bottinelli L., Durand N., Gouguenheim L., Paturel G., 1990, A&AS 86, 473

Paturel G., Bottinelli L., Gouguenheim L., Fouqué P., 1988, A&A 189, 1

Paturel G., Bottinelli L., Fouqué P., et al., 1990, The Messenger 62, 8

Paturel G., Bottinelli L., Di Nella H., et al., 1994, A&A 289, 711

Paturel G., Fouqué P., Bottinelli L., Gouguenheim L., 1989, A&AS 80, 299 and Extragalactic Database Monographs 1, Vols. 1-3

Roth J., Mould J., Staveley-Smith L., 1994, AJ 108, 851

Staveley-Smith L., 1985, PhD thesis, University of Manchester

Tully B., Fisher R., 1977, A&A 54, 661

Vaucouleurs G. de, Vaucouleurs A. de, Corwin H.G. Jr., 1976, Second Reference Catalogue of Bright Galaxies. University of Texas Press, Austin (RC2)

TABLE 1. The Table of 52 observed galaxies

PGC/LEDA	Name	R.A. 1950 DEC.	Vlit.	V20		W20		W50		F(HI)	S/N	Note
		h m s d ' "	km/s	km/s		km/s		km/s		Jy.km/s		
(1)	(2)	(3)	(4)	(5)		(6)		(7)		(8)	(9)	(10)
PGC 01532	ESO 242- 7	002155.0-454706	5720	5635	6	441	18	431	12	2.3	3.6	
PGC 02958	ESO 150- 24	004834.9-555248	7850	7911	8	431	24	415	16	5.8	3.5	
PGC 05764	ESO 13- 16	013238.0-794348	1795	1767	3	186	9	166	6	11.8	10.0	
PGC 05967	ESO 13- 18	013643.0-803606	4208	4322	9	291	25	260	17	6.0	4.5	
PGC 06249	NGC 2573	024256.1-893412	2278	2429	5	250	16	220	11	9.2	6.9	
PGC 08320	ESO 298- 15	020836.0-410912	1469	1415	5	181	14	157	10	10.0	7.1	
PGC 10624	ESO 299- 18	024632.0-404542	4801	4752	16	453	48	367	32	14.3	4.0	
PGC 14093	ESO 83- 12	035431.0-660518	5660	5474	30	540	89	404	59	6.6	2.7	
PGC 15790	ESO 84- 34	043956.9-631206	6275	6199	16	502	49	444	33	8.3	3.2	
PGC 15802	ESO 157- 50	043933.0-525106	3636	3871	8	225	25	204	17	7.2	3.8	
PGC 18355	NGC 2187A	060405.9-693524	3930	3964	14	464	43	417	29	3.9	3.3	
PGC 18407	ESO 307- 17	060448.9-395124	4990	4902	3	418	10	366	7	12.9	14.6	
PGC 20094	ESO 309- 17	070229.0-414818	5235	5240	8	469	24	437	16	8.4	4.9	
PGC 20865	ESO 123- 9	072215.0-615548	3406	3216	3	292	8	277	5	15.8	10.4	
PGC 21429	ESO 208- 31	073622.0-521124	3179	3068	7	370	22	351	15	7.1	4.1	
PGC 21472	ESO 59- 12	073834.0-683918	1345	1323	11	196	33	177	22	2.3	2.7	
PGC 21815	ESO 311- 12	074553.0-411936	1128	1131	12	239	36	215	24	2.7	2.8	(2)
PGC 26003	ESO 91- 3	091228.0-632512	1904	1906	3	344	9	330	6	14.1	9.1	
PGC 26532	ESO 126- 10	092108.0-605006	2074	2152	5	380	16	346	11	7.9	7.5	
PGC 28025	ESO 61- 15	094519.0-684100	4984	4885	4	379	12	356	8	25.5	8.1	
PGC 29450	ESO 316- 29	100540.0-410518	5701	5803	4	420	13	387	9	5.8	9.0	
PGC 29723	ESO 263- 16	101028.9-445924	4195	4116	1	211	3	191	2	16.9	28.0	
PGC 32660	ESO 264- 48	105034.0-452442	2847	2874	4	304	11	277	7	15.0	10.0	
PGC 35140	ESO 216- 8	112323.0-475200	5588	5570	6	453	18	436	12	11.6	4.6	
PGC 37334	ESO 320- 31	115134.0-393506	2947	2889	7	359	20	344	13	8.8	4.0	
PGC 38841	ESO 321- 10	120906.0-381612	3150	3147	7	359	21	326	14	4.5	5.6	
PGC 47003	ESO 220- 8	132304.9-475830	2977	2821	19	736	56	678	37	10.0	2.8	(3)
PGC 49586	NGC 5365A	135335.0-434548	2795	2760	8	426	24	406	16	4.6	3.8	
PGC 49655	ESO 174- 3	135419.0-523142	4027	4023	7	250	21	210	14	26.7	6.3	
PGC 50330	ESO 175- 1	140316.9-550712	3766	3792	9	622	27	581	18	9.7	4.9	
PGC 50798	ESO 271- 22	141018.9-451048	3080	3017	3	371	10	352	7	15.8	8.8	
PGC 53377	ESO 327- 32	145241.9-390006	7389	7564	1	83	4	63	3	13.2	22.3	
PGC 53527	NGC 5786	145540.9-414848	3034	2998	5	442	15	330	10	50.3	14.0	
PGC 53535	ESO 327- 39	145545.0-422254	2903	2917	2	388	7	366	5	42.7	13.8	
PGC 55256	ESO 329- 7	152651.9-382842	4645	4654	4	490	11	467	7	10.4	9.0	
PGC 58999	ESO 137- 42	164317.0-600336	3443	3265	4	271	11	251	7	17.7	8.3	
PGC 59880	ESO 138- 17	170916.0-590254	3624	3521	2	164	6	143	4	19.4	15.7	
PGC 61532	ESO 71- 4	180632.0-673854	3350	3343	4	264	11	245	8	11.2	8.0	
PGC 61712	ESO 182- 10	181421.9-544248	3548	3549	1	207	3	189	2	29.5	30.0	
PGC 61814	ESO 280- 13	181941.9-431012	6076	6027	4	569	11	513	7	27.5	14.0	
PGC 61850	ESO 335- 11	182136.0-385030	3710	3901	5	246	14	209	9	7.4	9.2	
PGC 61948	ESO 281- 1	182610.0-424718	6233	6262	9	540	28	481	19	10.7	5.7	(1)
PGC 62361	ESO 336- 13	184202.0-391400	4968	4902	3	384	10	370	7	15.4	7.5	
PGC 62411	ESO 336- 16	184350.9-414624	5910	5998	4	429	13	404	9	9.4	7.9	
PGC 62614	ESO 231- 11	185355.0-473700	5025	5057	4	378	11	357	8	5.2	8.3	
PGC 62908	ESO 282- 21	190908.0-460542	5367	5320	7	382	22	349	15	6.8	5.3	(1)

TABLE 1. continued

PGC/LEDA	Name	R.A. 1950 DEC.	Vlit.	V20		W20		W50		F(HI)	S/N	Note
		h m s d ' "	km/s	km/s		km/s		km/s		Jy.km/s		
(1)	(2)	(3)	(4)	(5)		(6)		(7)		(8)	(9)	(10)
PGC 63007	ESO 184- 51	191256.0-534724	7211	7205	8	542	22	475	15	16.3	7.5	
PGC 63064	IC 4843	191501.0-592406	3972	3975	11	170	33	145	22	2.3	3.1	
PGC 63241	NGC 6794	192439.0-390118	5980	6019	9	409	26	365	18	8.1	5.2	
PGC 63297	ESO 184- 74	192619.9-572312	5059	5059	12	487	36	413	24	31.9	4.9	
PGC 63509	ESO 142- 30	193619.0-600948	4246	4242	16	476	49	399	33	11.8	3.7	
PGC 64422	ESO 340- 8	201349.0-410442	2852	2837	3	258	8	248	5	8.2	8.3	
PGC 64423	IC 4986	201318.0-551124	2119	2168	3	196	8	174	5	11.3	11.9	
PGC 64464	NGC 6889	201503.0-540648	2554	2535	3	188	9	178	6	6.6	7.4	
PGC 10329	NGC 1073	024105.0+010955	1209	1208		92		75		72.0	71.0	(4)
PGC 40761	IC 3356	122421.6+115018	1101	1103		95		74		24.0	44.0	(4)

Note: 1) Bizarre spectrum
2) W50 uncertain
3) Uncertain
4) Calibrating galaxy

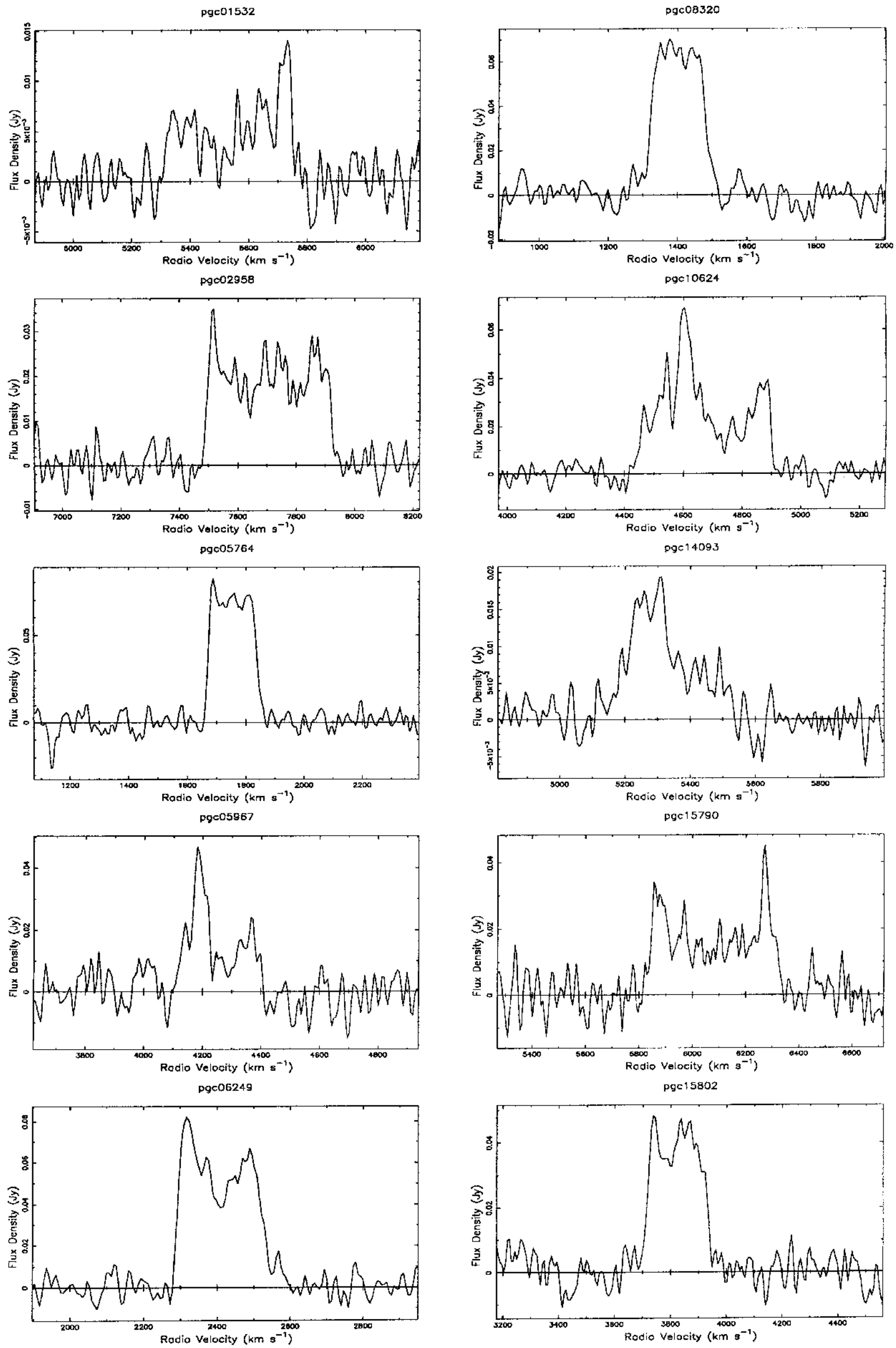
pgc01532
pgc08320
pgc02958
pgc10624
pgc05764
pgc14093
pgc05967
pgc15790
pgc06249
pgc15802
Flux Density (Jy)
Radio Velocity (km s^{-1})

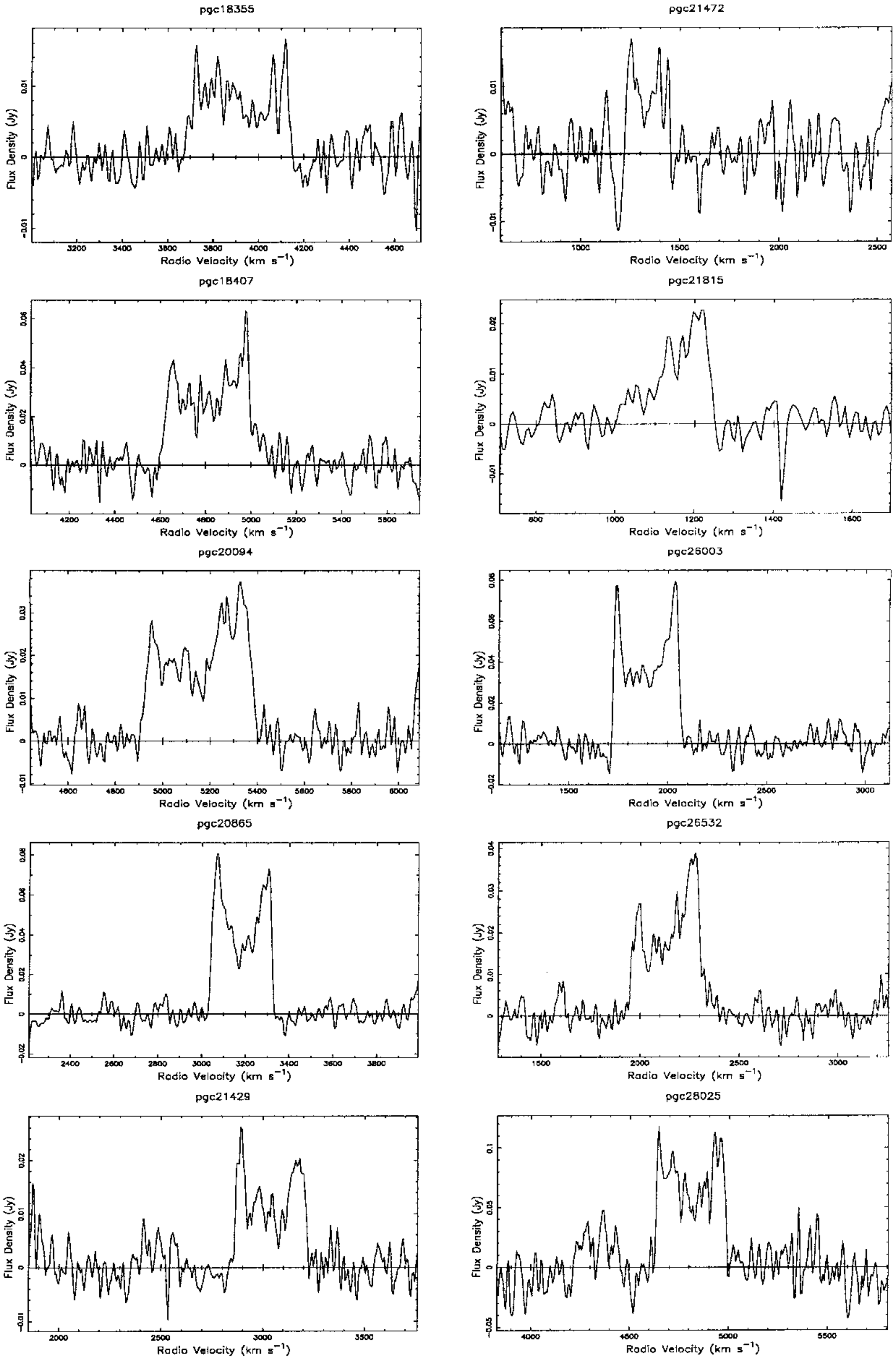
pgc18355
pgc21472
pgc18407
pgc21815
pgc20094
pgc26003
pgc20865
pgc26532
pgc21429
pgc28025
Flux Density (Jy)
Radio Velocity (km s^{-1})

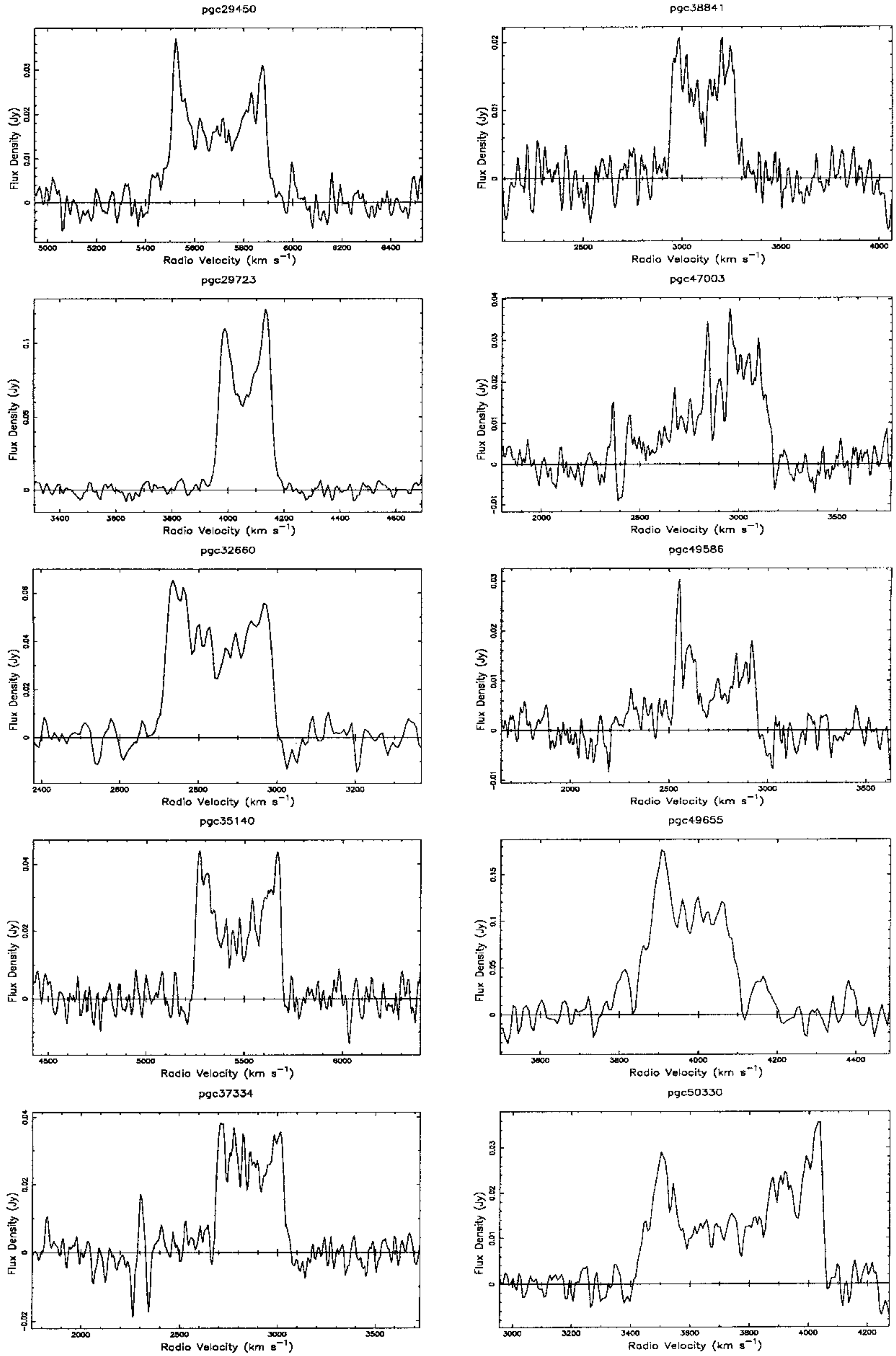
pgc29450
pgc38841
pgc29723
pgc47003
pgc32660
pgc49586
pgc35140
pgc49655
pgc37334
pgc50330
Flux Density (Jy)
Radio Velocity (km s^{-1})

pgc50798

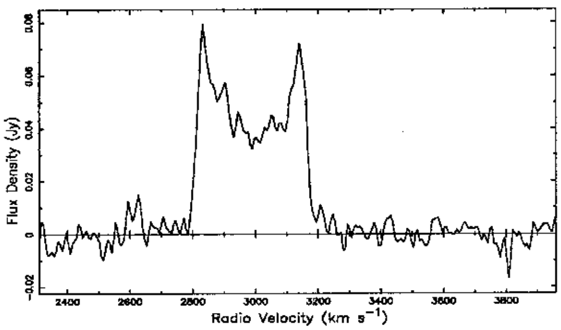

pgc53377

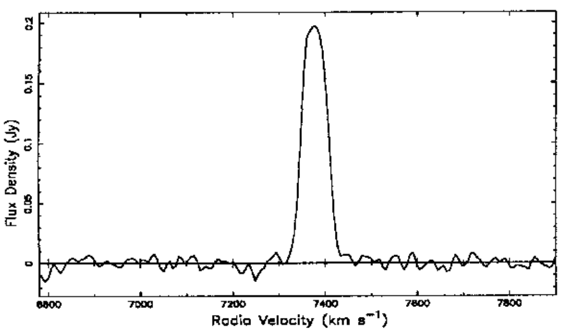

pgc53527

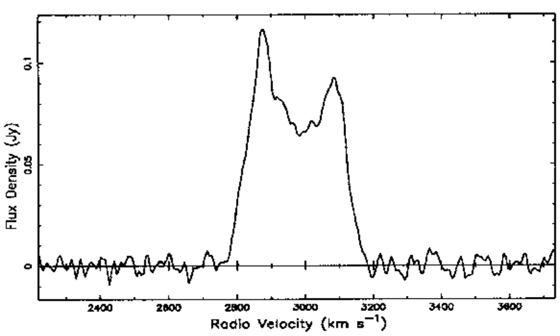

pgc53535

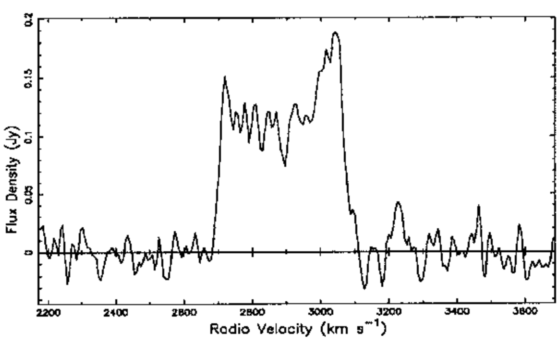

pgc55256

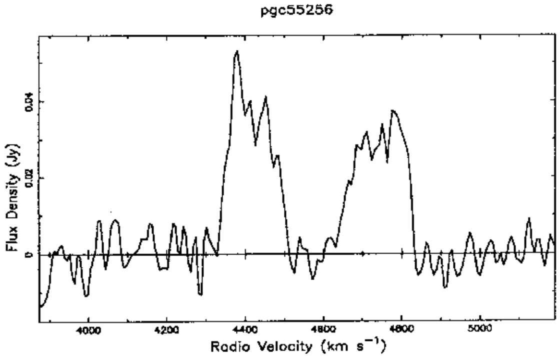

pgc58999

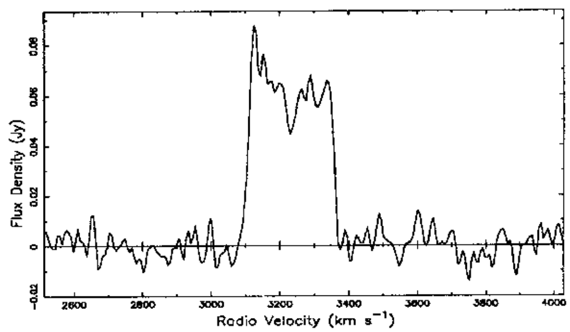

pgc59880

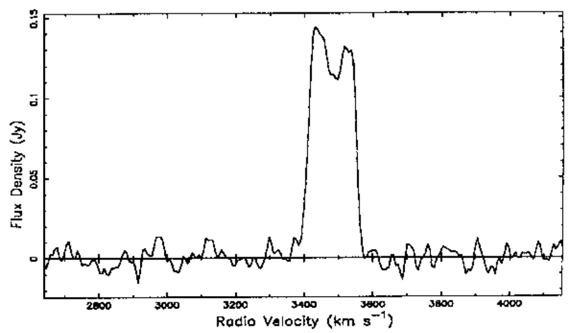

pgc61532

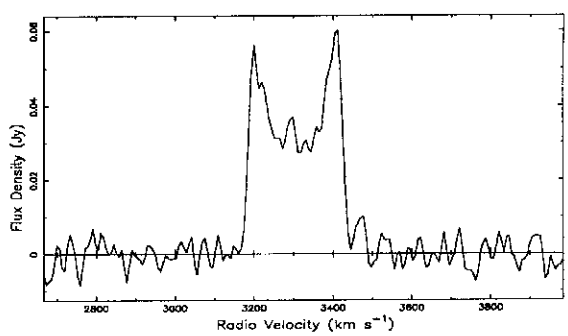

pgc61712

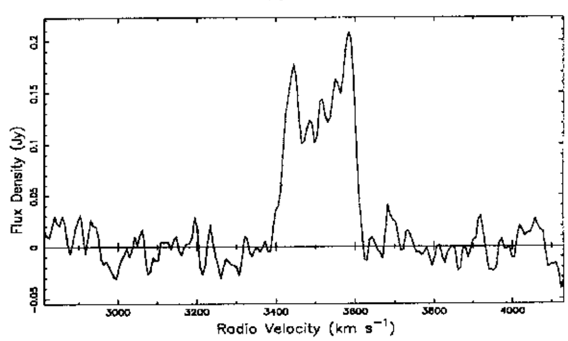

pgc61814

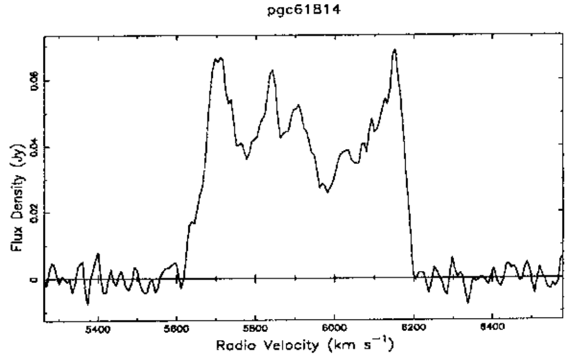

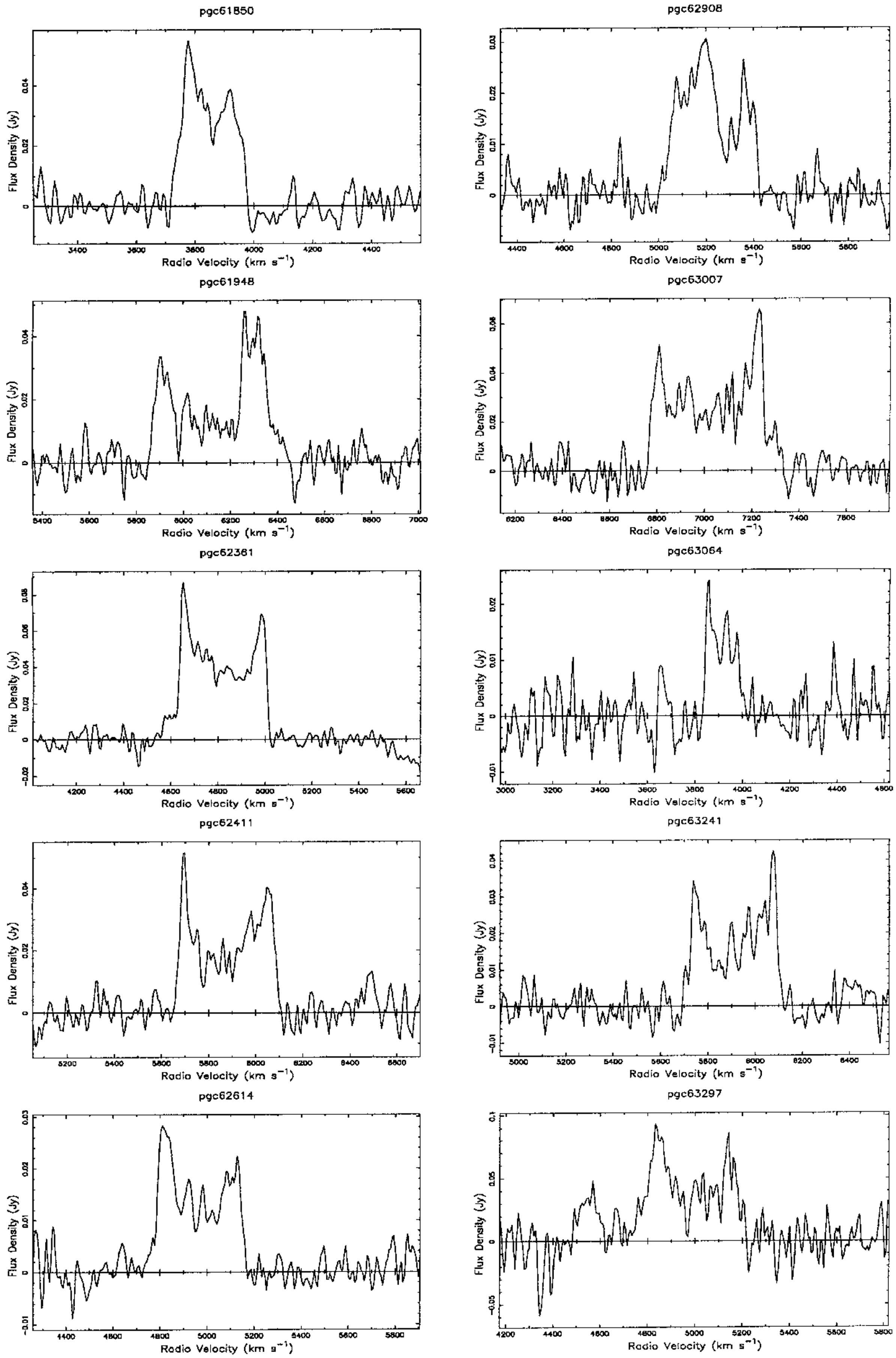
pgc61850
Flux Density (Jy)
Radio Velocity (km s⁻¹)
pgc62908
Flux Density (Jy)
Radio Velocity (km s⁻¹)
pgc61948
Flux Density (Jy)
Radio Velocity (km s⁻¹)
pgc63007
Flux Density (Jy)
Radio Velocity (km s⁻¹)
pgc62361
Flux Density (Jy)
Radio Velocity (km s⁻¹)
pgc63064
Flux Density (Jy)
Radio Velocity (km s⁻¹)
pgc62411
Flux Density (Jy)
Radio Velocity (km s⁻¹)
pgc63241
Flux Density (Jy)
Radio Velocity (km s⁻¹)
pgc62614
Flux Density (Jy)
Radio Velocity (km s⁻¹)
pgc63297
Flux Density (Jy)
Radio Velocity (km s⁻¹)

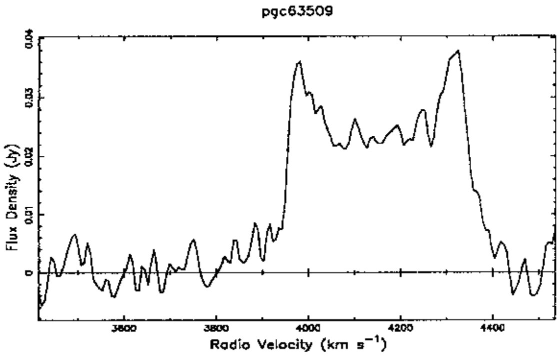
pgc63509
Flux Density (Jy)
Radio Velocity (km s⁻¹)

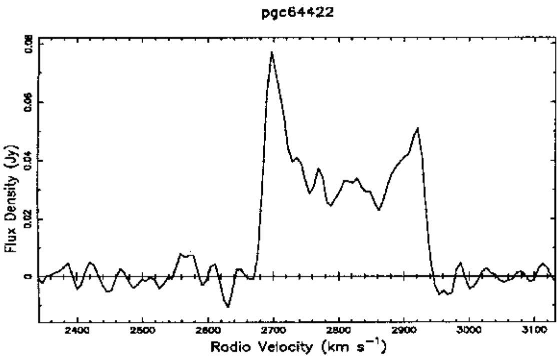
pgc64422
Flux Density (Jy)
Radio Velocity (km s⁻¹)

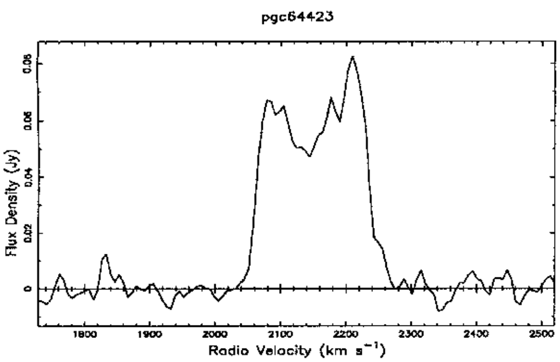
pgc64423
Flux Density (Jy)
Radio Velocity (km s⁻¹)

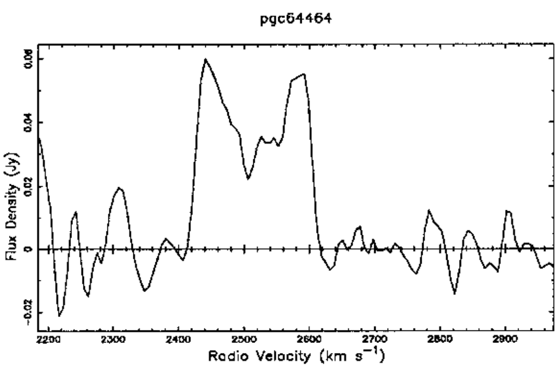
pgc64464
Flux Density (Jy)
Radio Velocity (km s⁻¹)